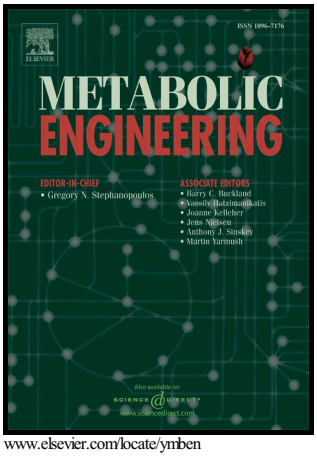

www.elsevier.com/locate/ymben

Enabling the synthesis of medium chain alkanes and 1-alkenes in yeast

Zhiwei Zhu, Yongjin J. Zhou, Min-Kyoung Kang, Anastasia Krivoruchko, Nicolaas A. Buijs, Jens Nielsen

PII: S1096-7176(17)30126-X
DOI: http://dx.doi.org/10.1016/j.ymben.2017.09.007
Reference: YMBEN1286

To appear in: *Metabolic Engineering*

Received date: 26 April 2017
Revised date: 11 September 2017
Accepted date: 13 September 2017

Cite this article as: Zhiwei Zhu, Yongjin J. Zhou, Min-Kyoung Kang, Anastasia Krivoruchko, Nicolaas A. Buijs and Jens Nielsen, Enabling the synthesis of medium chain alkanes and 1-alkenes in yeast, *Metabolic Engineering,* http://dx.doi.org/10.1016/j.ymben.2017.09.007

Enabling the synthesis of medium chain alkanes and 1-alkenes in yeast

Zhiwei Zhu[a,b], Yongjin J. Zhou[a,b,1], Min-Kyoung Kang[a,b,2], Anastasia Krivoruchko[a,b,3], Nicolaas A. Buijs[a,b,4], and Jens Nielsen[a,b,c,d,*]

[a] Department of Biology and Biological Engineering, Chalmers University of Technology, Kemivägen 10, SE-41296 Gothenburg, Sweden

[b] Novo Nordisk Foundation Center for Biosustainability, Chalmers University of Technology, SE-41296 Gothenburg, Sweden

[c] Novo Nordisk Foundation Center for Biosustainability, Technical University of Denmark, DK-2970 Hørsholm, Denmark

[d] Science for Life Laboratory, Royal Institute of Technology, SE-17121 Stockholm, Sweden

Present Addresses

1. Division of Biotechnology, Dalian Institute of Chemical Physics, CAS, Dalian, China

2. Department of Chemical and Biological Engineering, Northwestern University, Evanston, IL 60208, United States

3. Biopetrolia AB, Systems and Synthetic Biology, Chalmers University of Technology, SE-41296 Gothenburg, Sweden

4. Evolva Biotech, Lersø Parkallé 40-42, DK-2100, Copenhagen, Denmark

*. Correspondence to Jens Nielsen, E-mail: nielsenj@chalmers.se

Competing financial interests

The authors declare no competing financial interest.

Graphical abstract

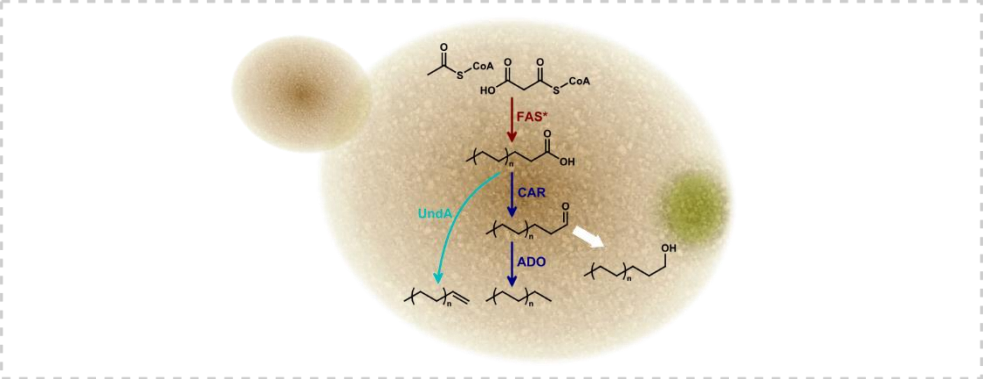

Abstract

Microbial synthesis of medium chain aliphatic hydrocarbons, attractive drop-in molecules to gasoline and jet fuels, is a promising way to reduce our reliance on petroleum-based fuels. In this study, we enabled the synthesis of straight chain hydrocarbons (C7–C13) by yeast *Saccharomyces cerevisiae* through engineering fatty acid synthases to control the chain length of fatty acids and introducing heterologous pathways for alkane or 1-alkene synthesis. We carried out enzyme engineering/screening of the fatty aldehyde deformylating oxygenase (ADO), and compartmentalization of the alkane biosynthesis pathway into peroxisomes to improve alkane production. The two-step synthesis of alkanes was found to be inefficient due to the formation of alcohols derived from aldehyde intermediates. Alternatively, the drain of aldehyde intermediates could be circumvented by introducing a one-step decarboxylation of fatty acids to 1-alkenes, which could be synthesized at a level of 3 mg/L, 25-fold higher than that of alkanes produced via aldehydes.

Keywords

Medium-chain fatty acids, alkanes, 1-alkenes, *Saccharomyces cerevisiae*

Highlights

1. Medium chain fatty acids were obtained by engineering fungal fatty acid synthases.
2. Medium chain alkanes were produced by expressing an alkane biosynthesis pathway.

3. Among 13 candidates, the ADO from *Thermosynechococcus elongatus* showed superior activity.
4. Targeting of the alkane-forming pathway into peroxisomes improved alkane production.
5. Medium chain 1-alkenes were synthesized by expressing UndA decarboxylase.

Abbreviations

MCFA, medium chain fatty acid; FAS, fatty acid synthase; Headspace/SPME/GC/MS, Headspace/solid-phase microextraction/gas chromatography/mass spectrometry; aldehyde deformylating oxygenase, ADO; carboxylic acid reductase, CAR.

1. Introduction

Medium chain aliphatic hydrocarbons (C7–C13) are the predominant components in petroleum-based gasoline or jet fuels (Edwards, 2003; Sheppard et al., 2016), and also serve as solvents and chemicals (Choi and Lee, 2013; Kourist, 2015). A variety of enzymes committed to the formation of hydrocarbons via the deoxygenation of fatty acids (Kourist, 2015; Rude et al., 2011; Rui et al., 2015; Rui et al., 2014) or fatty aldehydes (Aarts et al., 1995; Marsh and Waugh, 2013; Qiu et al., 2012; Schirmer et al., 2010) have been discovered in nature (Figure 1). In addition, the production of straight chain alkanes or 1-alkenes via biocatalysis (Amaya et al., 2016; Dennig et al., 2015; Foo et al., 2017; Liu et al., 2014; Yan et al., 2015; Zachos et al., 2015; Zhang et al., 2013) or heterologous biosynthesis (Akhtar et al., 2013; Bernard et al., 2012; Buijs et al., 2015; Cao et al., 2016; Chen et al., 2015; Choi and Lee, 2013; Coursolle et al., 2015; Foo et al., 2017; Harger et al., 2013; Howard et al., 2013; Kallio et al., 2014; Liu et al., 2014; Schirmer et al., 2010; Sheppard et al., 2016; Song et al., 2016; Xu et al., 2016; Yan et al., 2016; Zhou et al., 2016a; Zhou et al., 2016b) has been implemented. Yeast, an important industrial workhorse (Becker and Wittmann, 2015; Nielsen, 2015), is considered to be very suitable for the production of these fuel molecules (Hong and Nielsen, 2012). However, *in vivo* synthesis of medium

chain aliphatic hydrocarbons in yeast is not realized yet. This is mostly because of the scarcity of medium chain fatty acid (MCFA) precursors in native yeast cells. Recently, we have modified fungal type I fatty acid synthases (FASs) by inserting a heterologous thioesterase to release MCFAs and introducing mutations into the ketoacyl synthase domain (G1250S and M1251W in Fas2) to restrict the elongation of fatty acids (Gajewski et al., 2017a; Zhu et al., 2017). These modifications in FASs have allowed yeast to produce MCFAs. Here we further enabled the *in vivo* synthesis of medium chain alkanes and 1-alkenes in yeast by exploring the activities of hydrocarbon-forming enzymes towards medium chain substrates, and blocking the formation of by-products.

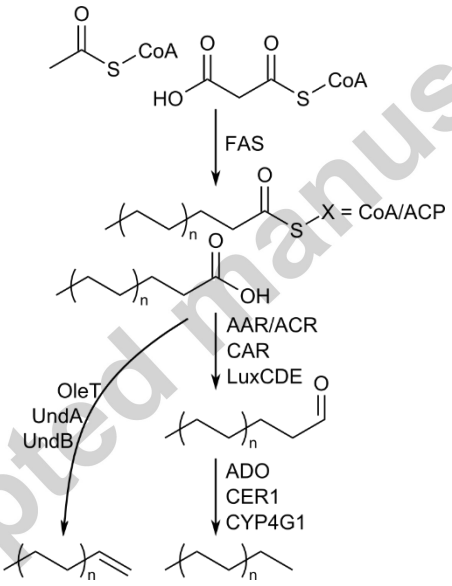

Figure 1. Biosynthetic pathways of straight chain aliphatic hydrocarbons. ACP, acyl carrier protein; CoA, coenzyme A; FAS, fatty acid synthase; AAR, acyl-ACP reductase; ACR, acyl-CoA reductase; CAR, carboxylic acid reductase; LuxCDE, fatty acid reductase complex components LuxC (reductase), LuxD (synthetase) and LuxE (transferase); ADO, cyanobacterial fatty aldehyde deformylating oxygenase; CER1, plant membrane-bound decarbonylase; CYP4G1, insect-specific P450 oxidative decarbonylase of the CYP4G family from *Drosophila*; OleT, P450 fatty acid decarboxylase; UndA, non-heme oxidase/decarboxylase; UndB, membrane-bound desaturase-like decarboxylase.

2. Materials and Methods

2.1. Plasmids, strains and culture conditions

Strains and plasmids used in this study were listed in Table S1 and Table S2, respectively. *E. coli* DH5α was used for plasmid amplification. If not specified, *E. coli* cells were cultivated in Luria-Bertani (LB) medium at 37 °C and 200 rpm. 80 mg/L of ampicillin was supplemented for plasmid selection. Transformation of *E. coli* was according to a previously described protocol (Inoue et al., 1990). All *S. cerevisiae* strains used in this study were derived from CEN PK113-11C (*MATa SUC2 MAL2-8c his3Δ1 ura3-52*). "YPD" medium (10 g/L yeast extract, 20 g/L peptone, and 20 g/L glucose) was used for regular culture of yeasts. "YPD+G418" medium containing 200 mg/L G418 (Formedium, Hunstanton, UK) was used for selection of transformants with a *kanMX* cassette. "SC-URA" medium containing 20 g/L glucose, 6.7 g/L yeast nitrogen base without amino acids (YNB, Formedium, Hunstanton, UK), and 0.77 g/L complete supplement mixture without uracil (CSM-URA, Formedium, Hunstanton, UK) was used for selection of transformants prototrophic to uracil. "SC+5FOA" medium containing 6.7 g/L YNB, 0.79 g/L complete supplement mixture (CSM, Formedium, Hunstanton, UK) and 0.8 g/L 5-fluoroorotic acid (5-FOA, Sigma-Aldrich) was used for recycling of *URA3* marker. 20 g/L agar (Merck Millipore) was added to make solid media. The recipe of Delft medium was described before (Jensen et al., 2014). 100 mg/L histidine and/or 100 mg/L uracil were supplemented as needed. If not specified, 20 g/L glucose was used as carbon source. Yeast cells were cultivated at 30 °C and 200 rpm in liquid media. A LiAc/SS carrier DNA/PEG method (Gietz and Schiestl, 2007) was used for yeast transformation. Cell density (OD at 600 nm) was measured by GENESYS 20 spectrophotometer (Thermo Fisher Scientific).

2.2. Plasmid and strain construction

Codon-optimized genes were synthesized by GenScript (Piscataway, NJ, USA) and listed in Table S3. Primers used in this study (Table S4) were synthesized by Sigma-Aldrich or Eurofins Genomics.

PrimeStar DNA polymerase (Takara Bio), Zymoprep Yeast Plasmid Miniprep II kit (Zymo Research Corp), Restriction enzymes, DreamTaq DNA Polymerase, DNA gel purification and plasmid extraction kits (Thermo Fisher Scientific), and Gibson Assembly Master Mix (New England BioLabs) were used according to the manufacturers' instructions. DNA sequencing was performed by Eurofins Genomics.

ADO and UndA-like genes were inserted into vectors pZWM1 (*TEF1* promoter and *ADH1* terminator) or pZWM2 (enhanced *TDH3* promoter and *CYC1* terminator) by using the Gibson assembly cloning kit and primers 1–36. Internal primer pairs (37–52 in Table S4) were used for introducing site-directed mutations into ADO genes. All plasmids were verified by sequencing.

The DNA assembler method (Shao et al., 2009; Zhou et al., 2012) was used for the construction of pAlkane261 and pAlkane262 plasmids, and primers 53–65 were used to amplify DNA fragments from pAlkane26 (Zhou et al., 2016a) or pZWM2-TeADO. A yeast 2μ vector pYX212 containing a *URA3* selection marker was used and linearized by digestion with restriction enzymes SphI and EcoRI. The PCR fragments accompanied with the linearized vector were transformed into *S. cerevisiae* YJZ02 and selected on "SC-URA" plates. Plasmids extracted from transformants by the Zymoprep Yeast Plasmid Miniprep II kit were transformed into *E. coli* DH5α. The plasmids extracted from *E. coli* were verified by restriction digestion and sequencing.

CRISPR/Cas9-mediated genome engineering was implemented by co-transformation of a repair fragment, and an all-in-one plasmid pECAS9-gRNA expressing high-fidelity Cas9 nuclease (eCas9) (Slaymaker et al., 2016) and guide RNA. The high-fidelity version of Cas9 was obtained by using primers 66–73 to introduce K848A, K1003A, and R1060A mutations into the TEF1p-Cas9-CYC1t cassette from p414-TEF1p-Cas9-CYC1t (DiCarlo et al., 2013). The guide RNA expression cassette (targeting *HFD1* gene) was obtained by using primers 74–77 and pROS10 (Mans et al., 2015) as DNA template. The 2μ vector backbone was amplified from pYX212 by using primers 78–79, and the *kanMX* and *KlURA3*

selection markers were amplified from pUG6 (Gueldener et al., 2002) and pWJ1042 (Reid et al., 2002), respectively, by using primers 80–83. The pECAS9-gRNA-KlURA3-tHFD1 and pECAS9-gRNA-kanMX-tHFD1 plasmids were generated by Gibson assembly cloning. The 100 bp repair fragment bridging a 50 bp upstream sequence and a 50 bp downstream sequence of the *HFD1* open reading frame was generated by PCR amplification with primers 84–85 which had a 20-bp overlap. For the construction of YJZ03 (*Δpox1* & *Δhfd1*) isogenic strain, 1 μg of pECAS9-gRNA-kanMX-tHFD1 and 200 ng of the repair fragment were transformed into YJZ02 (*Δpox1*), and "YPD+G418" plates were used for selection of transformants. While for the deletion of *hfd1* in ZW207 strain (*kanMX*$^{+}$), 1 μg of pECAS9-gRNA-KlURA3-tHFD1 and 200 ng of the repair fragment were used for transformation, and "SC-URA" plates were used for selection of transformants. Primers 86–87 were used for PCR verification of *hfd1* deletion. After confirmation of the deletion, the strains were cultivated in non-selective medium (YPD) to remove the corresponding plasmids.

ZW540 strain used for *in vivo* evaluation of ADO enzymes was constructed as described below. The *MmCAR*, *npgA*, *EcFd,* and *EcFNR* genes expressed in ZW540 were described previously (Zhou et al., 2016b). Primers 88–105 were used to generate cassettes for the integration of GAL7p-MmCAR-ADH1t and GAL3p-npgA-FBA1t into the *GAL1/10/7* locus. These cassettes were transformed into YJZ03 and selected on "SC-URA" plates. After colony PCR verification (Looke et al., 2011), the strain carrying correct integration cassettes was selected on "SC+5FOA" plates to recycle the *URA3* marker. Similarly, primers 106–121 were used to generate cassettes for the further integration of GAL1p-EcFNR-CYC1t and GAL10p-EcFd-TDH2t into the *GAL80* locus, and the strain obtained after removal of *URA3* marker was designated as YJZ54. *ScFAS27* was integrated into YJZ54 as described before (Zhu et al., 2017) to generate strain ZW540.

2.3. MCFA production

Delft medium with 100 mg/L histidine and 20 g/L glucose was used for the cultivation of YJZ02 (*Δpox1*) and YJZ03 (*Δpox1* & *Δhfd1*) carrying p*Sc*FAS28 plasmid, and Delft medium with 100 mg/L histidine, 100 mg/L uracil, and 20 g/L glucose was used for the growth of ZW207 and ZW2071. Single colonies were initially inoculated into 2 ml liquid medium and cultivated for 24 hours. The cells then grew in 100 ml shake flasks containing 20 ml medium with the initial OD of 0.1. After cultivation for 48 and/or 96 hours, one milliliter of culture broth was taken for extraction of extracellular fatty acids. Previously described methods (Zhu et al., 2017) were used for extraction, transesterification, and quantification of MCFAs.

2.4. Evaluation of aldehyde deformylating oxygenase (ADO) homologs

The plasmids expressing individual ADO genes were transformed into strain ZW540. Single colonies of each transformation were inoculated into 1 ml of Delft medium with 100 mg/L histidine and 5 g/L glucose in 14 ml culture tubes (17 × 100 mm, VWR) and cultivated for 24 hours. Then 200 µl of each pre-culture was transferred into 1.8 ml of the same medium in 20 ml headspace vials (75.5 × 23 mm, La-Pha-Pack GmbH, Langerwehe, Germany). The vials were tightly sealed with 18 mm magnetic precision thread screw caps (silicone/PTFE septa, 8 mm center hole, La-Pha-Pack GmbH). After cultivation at 30 °C and 200 rpm for 24 hours, the samples were directly analyzed by Headspace/Solid-Phase Microextraction/Gas Chromatography/Mass Spectrometry (Headspace/SPME/GC/MS). The OD was measured after GC/MS analysis.

A PAL COMBI-xt autosampler (CTC Analytics AG, Zwingen, Switzerland) was used for sample processing, and a FOCUS GC/ISQ single quadrupole MS system (Thermo Fisher Scientific) equipped with a ZB-50 column (30 m × 0.25 mm × 0.25 µm, Phenomenex Inc., UK) and a 0.8 mm i.d. inlet liner (SGE Analytical Science, Ringwood, Australia) was used for sample analysis. Helium (1 ml/min) was used as carrier gas. The sample vials were pre-incubated in the agitator at 50 °C for 10 seconds, and

the agitator was vigorously shaken at a speed of 500 rpm (in a pulsed mode, 5 seconds on and 2 seconds off). Then a polydimethylsiloxane fiber (PDMS, 30 μm, CTC Analytics AG) was inserted into the headspace to absorb the analytes for 10 seconds, and the analytes were desorbed from the fiber in a splitless injector of GC (260 °C and 10 seconds). The fiber was then post-conditioned at 280 °C for 10 seconds. The oven temperature was set at 40 °C for 2 minutes; increased to 140 °C at a rate of 10 °C/min, then increased to 300 °C at a rate of 20 °C/min with a subsequent incubation at 300 °C for 2 minutes. The temperature of MS transfer line and ion source were set at 250 °C and 200 °C, respectively. The fragment ions derived from electron ionization (70 eV) were detected in a full scan mode (50-450 m/z) and a selected ion monitoring mode (57 m/z). The compound identities were assigned through comparison with commercial standards and the NIST Mass Spectral Database. The area of the specific ion (57 m/z) was used for the quantification of alkanes and alcohols by calibration curves of each individual standards which were dissolved in methanol, and then added into 2 ml liquid medium in headspace vials and analyzed by the same method.

2.5. Comparison of cytosolic and peroxisomal alkane biosynthesis pathways

The plasmids expressing cytosolic or peroxisomal alkane biosynthesis pathways were transformed into host strains with different capacity of MCFA production. After cultivation in 1 ml Delft medium with 100 mg/L histidine and 5 g/L glucose for 24 hours, the cells were pelleted and resuspended in fresh medium and then inoculated into 2 ml medium in headspace vials with the initial OD of 0.1. The volatile metabolites were analyzed by Headspace/SPME/GC/MS as described above, after cultivation of the cells in headspace vials for 24 hours.

2.6. Medium chain 1-alkene synthesis

The plasmids expressing individual UndA-like genes were transformed into host strains producing MCFAs. For the evaluation of different UndA-like enzymes, transformants were inoculated into 1 ml

Delft medium with 100 mg/L histidine and 5 g/L glucose and cultivated for 24 hours. Then 200 µl of each pre-culture was inoculated into 1.8 ml liquid medium in headspace vials and then cultivated for 24 hours. For 1-alkene synthesis by Pput_3952 at different glucose concentration, inocula cultivated in 1 ml Delft medium with 100 mg/L histidine and 5 g/L glucose were pelleted and resuspended in fresh media with 5, 10 or 20 g/L glucose, respectively. Then the cells were inoculated into 2 ml corresponding media with the initial OD of 0.1. After cultivation in headspace vials for 24 hours, the volatile metabolites were analyzed by above mentioned Headspace/SPME/GC/MS with minor modification. The fragment ions were detected in a full scan mode (50-450 m/z) and a selected ion monitoring mode (55 m/z). Area of the specific ion (55 m/z) was used for the quantification of 1-alkenes by calibration curves of each individual standards.

2.7. Quantification of protein expression levels

Cells cultivated in 2 ml Delft medium with 100 mg/L histidine and 5 g/L glucose for 24 hours were used for protein extraction. The cell pellets harvested from 1 OD of culture broth were treated with NaOH and SDS-PAGE sample buffer as previously described (Kushnirov, 2000). The supernatant thereof was diluted 4 times with SDS-PAGE sample buffer, and the protein samples (6 µl) were loaded into 12% Mini-PROTEAN® TGX™ Precast Protein Gels (Bio-Rad). The Spectra™ Multicolor Broad Range Protein Ladder (Thermo Fisher) was used as protein molecular weight standards. Electrophoresis was carried out at room temperature at 150 V for 55 min with a Mini-PROTEAN Tetra Cell electrophoresis apparatus (Bio-Rad). The gels were then treated with fixation buffer (45% ethanol and 10% acetic acid in MilliQ H_2O) for 30 min, washed with deionized water for 5 min, stained with Bio-Safe™ Coomassie Stain (Bio-Rad) for 60 min, and destained with deionized water for 3 hours. The Image Lab software (Bio-Rad) was used for protein quantification based on gel band intensities.

3. Results and discussion

3.1. Medium chain fatty acid production

Although MCFAs are valuable precursors for the synthesis of oleochemicals and biofuels, very few of them are generated by native FASs. Recently, we and others have engineered fungal type I FASs for MCFA production (Gajewski et al., 2017b; Xu et al., 2016; Zhu et al., 2017). By embedding a heterologous short chain acyl-ACP/CoA thioesterase into the reaction compartments of FAS, as well as introducing mutations into the ketoacyl synthase domain, the engineered *Sc*FAS28 produced substantial MCFAs in *Δpox1* strains (Figure 2, also see ref. (Zhu et al., 2017)). Hfd1 is an aldehyde dehydrogenase involved in both sphingolipid degradation (Nakahara et al., 2012) and coenzyme Q biosynthesis (Payet et al., 2016; Stefely et al., 2016). Hfd1 deficiency could eliminate the oxidation of fatty aldehydes to fatty acids, which has been shown to be crucial for alkane synthesis (Buijs et al., 2015; Zhou et al., 2016a; Zhou et al., 2016b). Interestingly, deletion of *hfd1* significantly augmented MCFA production (Figure 2a and 2c). Due to higher biomass levels of the *Δhfd1* strains (Figure 2a and 2b) and the toxicity of MCFAs to yeast cells (Liu et al., 2013), we speculated that *hfd1* deletion improved the cell fitness against these toxic products, and we found that *hfd1* deletion partially relieved the growth arrest resulting from octanoic acid stress (Figure S1). Although we did not further dissect the mechanism of improved tolerance to MCFAs in *Δhfd1* cells, the results here showed that improvement in cell fitness could facilitate the production of toxic MCFAs.

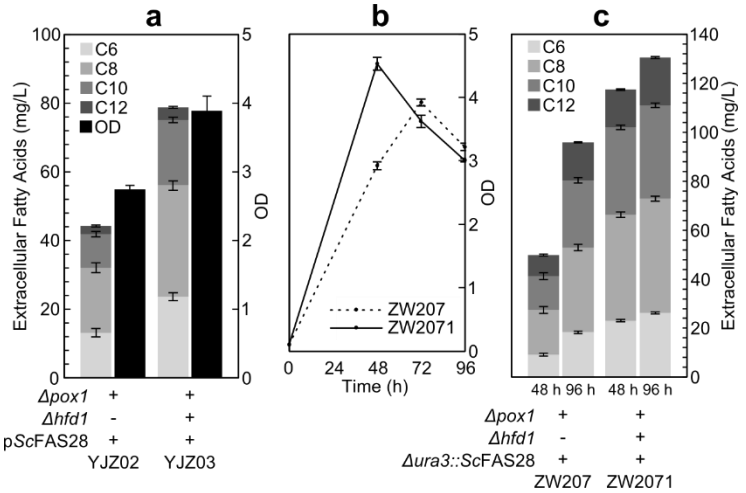

Figure 2. Medium chain fatty acid production. (**a**) Extracellular fatty acids and final cell mass represented as optical density (OD) at 600 nm produced by strains YJZ02 (*Δpox1*) and YJZ03 (*Δpox1* and *Δhfd1*) expressing an engineered FAS via the plasmid p*Sc*FAS28. Cells were cultivated in "Delft + Histidine" medium for 48 hours. (**b**) Growth of ZW207 (*Δpox1* and *Δura3*::*ScFAS28*) and ZW2071 (*Δpox1*, *Δhfd1* and *Δura3*::*ScFAS28*) in "Delft + Histidine + Uracil" medium. OD was measured after inoculation for 48, 72 and 96 hours. (**c**) Extracellular fatty acids produced by strains ZW207 and ZW2071 after cultivation for 48 and 96 hours as shown in (b). Mean ± standard deviation of four replicates is presented.

3.2. Screening ADOs for medium chain alkane synthesis

As MCFAs could be produced *in vivo* by engineered FASs (Figure 2 and ref. (Zhu et al., 2017)), we next focused on optimizing the downstream alkane biosynthesis pathway for medium chain alkane production. Our previous studies have shown that the expression of a heterologous alkane biosynthesis pathway consisting of a carboxylic acid reductase (CAR) and a cyanobacterial ADO (Figure 1) enabled the synthesis of long chain alkanes (Zhou et al., 2016a; Zhou et al., 2016b). The CAR enzyme used in this pathway is superior, since its substrates, free fatty acids, are more available than fatty acyl-CoA (Zhou et al., 2016b). Moreover, this enzyme displays good activity towards MCFAs (Akhtar et al., 2013; Finnigan et al., 2016). However, higher catalytic activity and better substrate preference to medium chain aldehydes are desired for the ADO enzyme. This drove us to screen different ADO orthologs and engineer their substrate binding sites in order to obtain more appropriate candidates.

We constructed a stable host strain ZW540 in which the *POX1* and *HFD1* were deleted, and components of the alkane biosynthesis pathway, including engineered FAS, CAR, phosphopantetheinyl transferase NpgA, ferredoxin and ferredoxin-$NADP^+$ reductase, were integrated into the

chromosomes. The ADO activity towards medium chain substrates could be readily evaluated through quantification of alkanes produced by strain ZW540 harboring a plasmid expressing the ADO gene (Figure 3a). We then expressed a previously described ADO from *Synechococcus elongatus* (*Se*ADO) (Buijs et al., 2015; Zhou et al., 2016a; Zhou et al., 2016b) in ZW540. As the medium chain alkanes are highly volatile chemicals, we cultivated the cells in tightly sealed headspace vials to prevent the loss of volatile products. Two milliliters of liquid medium containing 5 g/L glucose in 20 ml vials was used for cell culture. Limited glucose feeding enabled aerobic cell metabolism, as well as induced the expression of heterologous genes controlled by GAL promoters (Nehlin et al., 1991; Pannala et al., 2010). After cultivation for 24 hours, four odd-chain alkane molecules (C7–C13), which were derived from corresponding even-chain fatty acids (C8–C14), were detected by Headspace/SPME/GC/MS analysis (Figure S2). We did not find myristic acid during the measurement of extracellular fatty acids (Figure 2), as little myristic acid was secreted out by our engineered strains. The tridecane production, however, indicated that myristic acid produced in the cells was used as a substrate for alkane synthesis. The successful detection of medium chain alkanes showed that our system for *in vivo* evaluation of ADO enzymes worked well.

Khara *et al*. previously substituted two residues (V41 and A134) of the ADO from *Prochlorococcus marinus* (*Pm*ADO) with tyrosine or phenylalanine to introduce steric restriction into the binding cavity of long chain aldehydes (Figure S3a-c, (Khara et al., 2013)). Due to the high sequence identity among ADOs (Figure S3a) and the superposed structures between *Se*ADO and *Pm*ADO (Figure S3d), we introduced the V28Y and A121F mutations (equivalent to V41Y and A134F in *Pm*ADO, respectively) into *Se*ADO, and expressed these two mutants in ZW540 strain. Interestingly, we did not find increased production of medium chain alkanes by the V28Y mutant of *Se*ADO, however, the heptane and

undecane produced by the A121F mutant of *Se*ADO increased approximately 100% compared with those produced by wild type *Se*ADO (Figure S4).

We then introduced the similar mutation (equivalent to V121F in *Se*ADO) into 13 other ADO orthologs, and expressed these mutants along with the wild type ADOs, resulting in expression of 28 ADO proteins in ZW540 strain. Among these ADOs, detailed biochemical and structural properties of *Se*ADO and *Pm*ADO have been characterized before (Jia et al., 2015; Khara et al., 2013). *Np*ADO has been reported previously having better *in vivo* activity than *Se*ADO and *Pm*ADO for long chain alkane synthesis in *E. coli* (Schirmer et al., 2010). *Te*ADO is from thermophilic cyanobacterium *Thermosynechococcus elongatus* BP-1 and probably has a more stable protein structure. Other ADOs are from diversified cyanobacterial species. All these ADO proteins share high identity in sequence, and have conserved residues for coordinating di-iron cofactors (Figure S3a and 3b). Homology modeling shows that they share a structure with 8 α-helices, among which a four-helix bundle (α1, α2, α4, and α5) provides the coordinating residues for binding of the di-iron cofactors (Figure S3b and 3d). Moreover, the residues (equivalent to V41 and A134 in *Pm*ADO) contributing to substrate chain length control are highly conserved as well (Figure 3a and 3c).

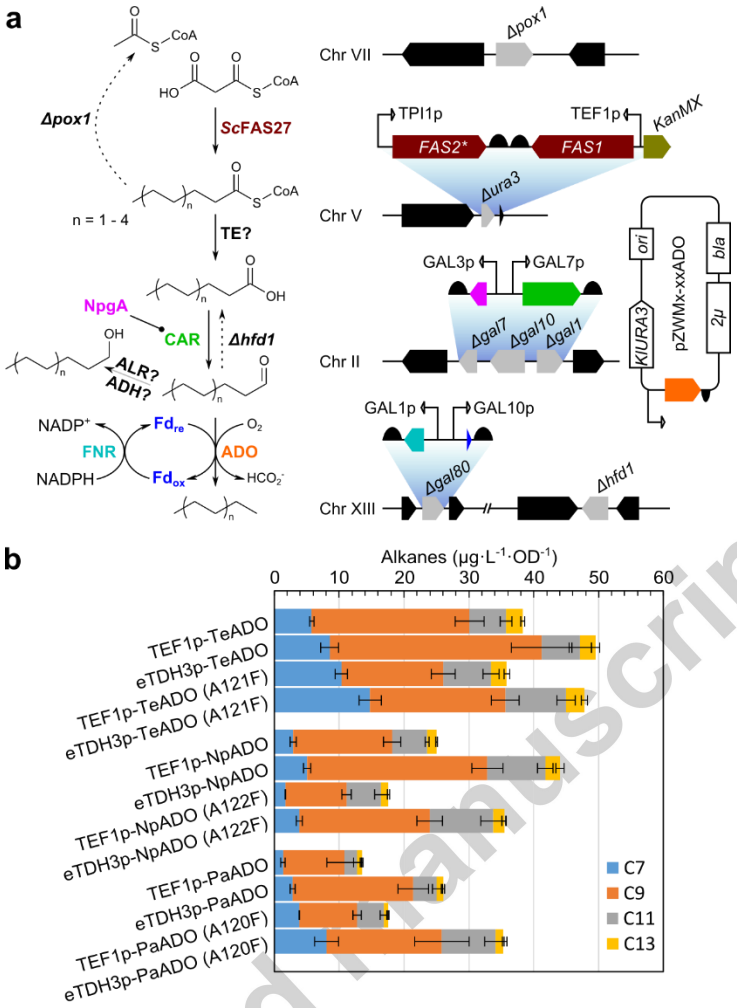

Figure 3. Medium chain alkane synthesis in yeast. (**a**) Genetic manipulations for medium chain alkane synthesis in ZW540 strain. The engineered *Sc*FAS27 with G1250S and M1251W mutations in Fas2 was expressed to generate medium chain fatty acids. *POX1* and *HFD1* genes were deleted to avoid reverse reactions. Carboxylic acid reductase (CAR) and its activation protein phosphopantetheinyl transferase NpgA were expressed to reduce fatty acids to aldehydes. Electron transfer system was composed of ferredoxin (Fd) and ferredoxin-$NADP^+$ reductase (FNR) from *E. coli*. Fatty aldehyde deformylating oxygenase (ADO) was expressed by a 2μ episomal plasmid. TE, thioesterase; ADH, alcohol dehydrogenase; ALR, aldehyde reductase. (**b**) Medium chain alkane production in ZW540 strain expressing ADOs from *TEF1* promoter (TEF1p) or enhanced *TDH3* promoter (eTDH3p). Cells were

cultivated in 20 ml tightly sealed headspace vials with 2 ml "Delft + Histidine" medium containing 5 g/L glucose for 24 hours. Mean ± standard deviation of three replicates is presented.

Next, we quantified the alkane production by comparison with commercially available standards and found only seven ADO enzymes had pronounced activities (Table S5). The medium chain alkane production varied up to 3-fold in yeast cells expressing different wild type ADO enzymes. However, the titers of medium chain alkanes were not correlated with the ADO protein levels (Figure S5), showing that the *in vivo* activities of ADOs were dependent on not only protein abundance, but also their affinities to electron donors or di-iron co-factors, as well as protein stability and aggregation status. Introducing the mutation into four ADOs (*Cw*ADO, *Se*ADO, *Pa*ADO, and *Te*ADO) resulted in increases of the total amount of medium chain alkanes. Among these medium chain alkanes, heptane and undecane were the most significantly elevated products. For *Pm*ADO, although the A134F mutant produced 48% more heptane than the wild type, the total amount of all four alkanes decreased by 44% compared with the wild type. Furthermore, the mutation in *La*ADO and *Np*ADO resulted in decreased production of all four alkanes. Although the previous study showed that the protein expression level of *Pm*ADO A134F mutant in *E. coli* was about 2-fold lower than that of the wild type (Khara et al., 2013), we did not observe significant variance in protein expression levels between ADO wild type and mutants (Figure S5).

Based on the extensive screening of ADO orthologs and mutants, we found that three ADO enzymes (*Te*ADO, *Np*ADO and *Pa*ADO) had superior *in vivo* activities for medium chain alkane synthesis. We then tried to increase the expression levels of these ADOs by using a hybrid *TDH3* promoter with tandem upstream activation sequences of *TEF1*, *CIT1* and *CLB2* genes (Blazeck et al., 2012; Zhou et al., 2016b). Elevated alkane production was found in the strains expressing ADOs by this enhanced *TDH3*

promoter (eTDH3p, Figure 3b). In the strains expressing *Np*ADO or *Pa*ADO, alkane titers increased by roughly 100% due to the use of eTDH3p compared to the *TEF1* promoter. The alkane production was less significantly improved (30%) when expressing *Te*ADO under the control of eTDH3p compared to the TEF1 promoter, probably because the basic synthesis of alkanes via expression of *Te*ADO from the *TEF1* promoter was relatively high. Together, we successfully elevated the medium chain alkane production by 250% through the expression of *Te*ADO under the control of eTDH3p compared with the initial expression of *Se*ADO under the *TEF1* promoter.

The currently available alkane biosynthesis pathway consists of two reactions, reduction of fatty acids or fatty acyl-CoA/ACP thioesters to aldehydes and decarbonylation of aldehydes to alkanes (Figure 1). In yeast cells, there are plenty of alcohol dehydrogenases and aldehyde reductases which could divert the aldehyde intermediates to alcohols (Figure 3a). The production of medium chain fatty alcohols in strain ZW540 indicated the activities of endogenous alcohol-forming enzymes (Figure S6). Similar to previous studies (Buijs et al., 2015; Zhou et al., 2016a; Zhou et al., 2016b), the fatty alcohols were the predominant products even in the strain expressing *Te*ADO under the control of eTDH3p (Figure S7), which showed again that the catalytic efficiency of ADO was not competitive to that of the alcohol-forming enzymes.

3.3. Compartmentalization of alkane biosynthesis pathway into peroxisomes

Through the expression of the alkane biosynthesis pathway in the cytosol (Figure 3), we enabled medium chain alkane production in yeast. However, substantial amounts of alcohol by-products derived from fatty aldehyde intermediates were formed (Figure S7). Recently, we have demonstrated that the compartmentalization of alkane biosynthesis pathway into peroxisomes could relieve the alcohol formation and provide a more suitable environment for alkane biosynthesis (Zhou et al., 2016a). Here we also used this strategy for medium chain alkane synthesis (Figure 4a).

Firstly, the cytosolic (pAlkane06) or peroxisomal (pAlkane26) alkane biosynthesis pathways were expressed in ZW202, a strain generating MCFAs at a moderate level (Zhu et al., 2017). Compared to the cytosolic pathway, the peroxisomal pathway yielded about 100% more medium chain alkanes, among which the nonane and undecane were the most significantly increased molecules (Figure 4b). Concurrently, the fatty alcohol formation in the strain expressing the peroxisomal alkane biosynthesis pathway decreased (Figure S8a), which was consistent with our previous work (Zhou et al., 2016a) and showed that the peroxisomal membrane provided a barrier to partially isolate aldehyde intermediates from cytosolic alcohol-forming enzymes. Next, we introduced both pathways into ZW207 that produced more MCFAs than ZW202 (Zhu et al., 2017). We found that the peroxisome compartmentalization in this strain also promoted alkane production (133%) compared with the cytosolic pathway. Moreover, ZW207 produced 12% more alkanes than ZW202 when the peroxisomal pathway was expressed (Figure 4b).

Hfd1 deficiency has been found to be beneficial for both MCFA (Figure 2) and long chain alkane production (Buijs et al., 2015; Zhou et al., 2016a; Zhou et al., 2016b), surprisingly, *hfd1* deletion did not improve medium chain alkane production (Figure 4b) even though significantly more aldehyde intermediates accumulated in ZW2071 expressing either alkane biosynthesis pathways (Figure S8b). We reasoned that the reducing equivalents for alkane synthesis were limited as most of them would be consumed during conversion of aldehydes to alcohols (Figure S8b). Nevertheless, peroxisome targeting of the alkane biosynthesis pathway elevated alkane production by 63% compared with the cytosolic pathway in ZW2071 (Figure 4b).

Since the activity of *Te*ADO for medium chain alkane synthesis is better than that of *Se*ADO, and increasing the expression level of *Te*ADO by eTDH3p was demonstrated promotion of alkane production (Figure 3b), we also utilized *Te*ADO for the peroxisomal conversion of aldehydes to alkanes

(pAlkane261 and pAlkane262 in Figure 4a). Although more heptane was obtained by using *Te*ADO, the total amount of all four medium chain alkanes did not change significantly. Given the high local concentration of these enzymes in the tiny space of peroxisomes, the availability of substrates and co-factors rather than the ADO activity is probably the most pivotal aspect controlling the flux of peroxisomal alkane synthesis.

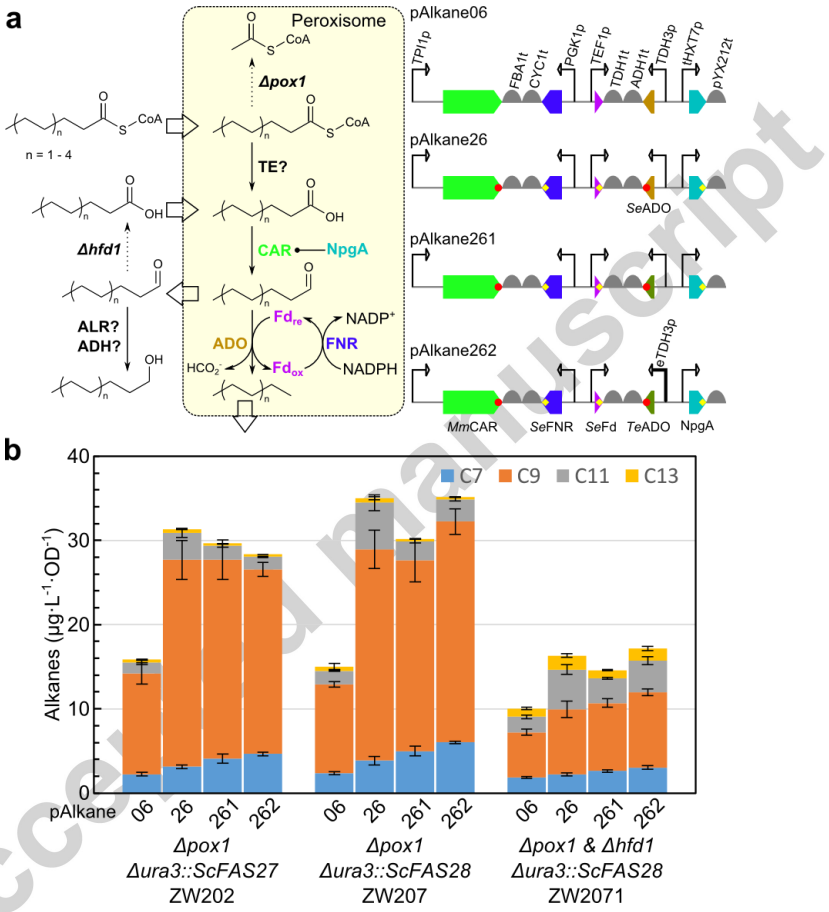

Figure 4. Compartmentalization of the alkane biosynthesis pathway into peroxisomes improved medium chain alkane production. (**a**) Schematic representation of the location of enzymes involved in alkane biosynthesis (left panel) and the plasmids for expression of alkane biosynthesis pathway (right panel). Two different peroxisomal targeting tags (per1, GGGSSKL, yellow diamonds; per2, GGGSAAVKLSQAKSKL, red circles) were fused to the C-terminus of enzymes to target the proteins into peroxisomes. (**b**) Quantification of medium chain alkanes produced by the strains carrying cytosolic or

peroxisomal alkane biosynthesis pathways. Cells were cultivated in headspace vials with 2 ml "Delft + Histidine" medium containing 5 g/L glucose for 24 hours. Mean ± standard deviation of four replicates is presented.

3.4. Medium chain 1-alkene biosynthesis by UndA

The alkane biosynthesis pathway consists of two reactions, of which the decarbonylation reaction catalyzed by ADO is of low efficiency. The poor catalytic activity of ADO is associated with the labile structure of its di-iron active center, which only enables 3-5 turnovers (Andre et al., 2013; Das et al., 2011; Eser et al., 2011; Jia et al., 2015; Warui et al., 2011). Moreover, the aldehyde intermediates are diverted into alcohols due to numerous endogenous aldehyde reductases or alcohol dehydrogenases in yeast (Zhou et al., 2016a; Zhou et al., 2016b). It is impractical to eliminate all these competitive alcohol-forming enzymes (Kallio et al., 2014; Sheppard et al., 2016; Zhou et al., 2016b), and the alternative strategy of compartmentalizing the alkane biosynthesis reactions into peroxisomes therefore improved medium chain alkane production (Figure 4). Additionally, the one-step decarboxylation of fatty acids to 1-alkenes avoids the formation of aldehyde intermediates. For instance, a recently discovered non-heme iron oxidase UndA (PFL_4321) catalyzes the O_2 dependent decarboxylation of fatty acids to the corresponding n-1 terminal alkenes (Figure 5a and ref. (Rui et al., 2014)). Importantly, steric restriction imposed by the bulky side chains of three amino acid residues (Y41, F239 and L240) in UndA limits the chain length of fatty acids (Figure S9 and ref. (Rui et al., 2014)), which renders the UndA enzyme the preference to medium chain substrates (C10–C14).

Eight UndA homologs were selected and codon-optimized for expression in yeast. All of these UndA orthologs have conserved Fe(II) coordinating amino acid residues equivalent to E101, H104 and H194 in UndA (Figure S9a). The amino acid residues responsible for substrate chain length specificity are less

conserved among the UndA homologs from species other than *Pseudomonas* (Figure S9a-c). Similarly, homology modeling showed a highly conserved structure between UndA orthologs (Figure S9d). We initially expressed PFL_4321 and Pput_3952 in ZW202 strain, and three odd-chain 1-alkenes (C7–C11) were detected (Figure S10). Although it was reported that the UndA failed to convert octanoic acid to 1-heptene (Rui et al., 2014), here we surprisingly found it did have such an activity. In contrast to the detectable tridecane during alkane biosynthesis (Figure 4b), we did not observe the 1-tridecene product in the same host strain, which suggested that the UndA had very poor activity towards myristic acid in *S. cerevisiae*. We then quantified the 1-alkene production in strain ZW207 expressing different UndA-like enzymes and found only four of them could produce 1-alkenes above the detection limit (Figure 5b). The expression of two enzymes, Pput_3952 and PFL_4321, resulted in the highest production of 1-alkenes. Moreover, Pput_3952 had better *in vivo* activity for 1-alkene synthesis than PFL_4321, which was consistent with previous work in *E. coli* (Rui et al., 2014). In addition, NJ69_11810 also showed minor activity, and Mpe_A3582 could produce 1-nonene product.

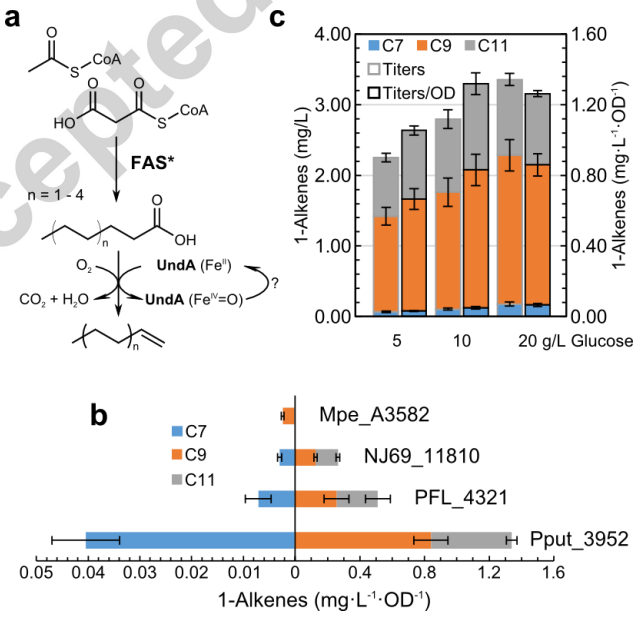

Figure 5. Medium chain 1-alkene synthesis. (**a**) Pathway for medium chain 1-alkene biosynthesis. Regeneration of UndA by reductive co-substrates was unclear (as shown by the question mark). (**b**) 1-

alkenes produced by ZW207 strain expressing different UndA-like enzymes. “Delft + Histidine” medium with 5 g/L glucose was used. (**c**) Increase 1-alkene production in ZW2071 strain expressing Pput_3952 by elevated feeding of carbon source. Cells were cultivated in headspace vials with 2 ml “Delft + Histidine” medium for 24 hours. Mean ± standard deviation of 3-4 replicates is presented.

We then expressed Pput_3952 in strain ZW2071, our best producer of MCFAs. 2.25 mg/L of 1-alkenes were produced when 5 g/L of glucose was fed. By feeding 20 g/L glucose, the titer increased further to 3.35 mg/L (1.25 $mg \cdot L^{-1} \cdot OD^{-1}$), which was 25-fold higher than that of alkanes (Figure 5c). These results showed the superiority of the one-step conversion of fatty acids to 1-alkenes via UndA compared with the two-step alkane biosynthesis. Consistently, only small quantities of volatile by-products, fatty acid ethyl esters, were formed due to the accumulation of ethanol when the glucose was fed at a high concentration (Figure S11).

According to the catalytic mechanism of UndA, Fe(IV)=O species formed during 1-alkene release have to be regenerated to enable multiple turnover reactions (Figure 5a and also ref. (Rui et al., 2014)). Although the natural reductive co-substrates in *Pseudomonas* were not discovered yet, a few reductants were found to enable multiple turnovers *in vitro* (Rui et al., 2014). Among these potential reductive co-substrates tested, ascorbate displayed the best performance in terms of 1-alkene production. In yeast, the biosynthesis of D-erythroascorbic acid (Hancock et al., 2000), an analog with similar redox properties as L-ascorbate (Shao et al., 1993), from D-arabinose is similar to the last two steps of plant L-ascorbate synthesis pathway (Figure S12a). Moreover, the intracellular accumulation of D-erythroascorbic acid and L-ascorbic acid in yeast was reported if D-arabinose and L-galactose were fed, respectively (Hancock et al., 2000). We therefore quantified the 1-alkenes produced by cells cultivated in media supplemented with L-galactose or D-arabinose, but we did not find any significant

difference in 1-alkene production (Figure S12b). Interestingly, the 1-alkene production decreased by 32% when 2 mM L-ascorbate was directly added to the medium (Fig. S12c). These results might indicate that ascorbate-like antioxidants seem not to be the intrinsic co-factors of UndA, and further studies to find out the appropriate reductive co-substrates, or to reconstruct a suitable enzyme reaction cascade enabling multiple turnovers will benefit the *in vivo* production of medium chain 1-alkenes.

Currently, three kinds of enzymes catalyzing one-step 1-alkene synthesis have been reported (Figure 1). However, there were only a few studies using yeast as the host for 1-alkene production. 3.7 mg/L (ca. 0.17 $mg \cdot L^{-1} \cdot OD^{-1}$) of long chain terminal alkenes were produced by an extensively engineered yeast strain with the cytochrome P450 oxidase OleT under fed-batch cultivation in bioreactors (Chen et al., 2015). About 0.2 mg/L of long chain 1-alkenes were obtained by the compartmentalization of OleT and the electron transfer system (flavodoxin and flavodoxin reductase) into peroxisomes of a yeast producing high levels of free fatty acids (Zhou et al., 2016a). In this work, a comparable amount of medium-chain 1-alkenes was produced via expression of the MCFA-preferring UndA in yeast under simple cultivation in vials (Figure 5), and further improvement in titer would be realized through, for example, providing an effective co-factor regeneration system for multiple turnover reactions, or optimizing culture mode in bioreactors for oxygen supply and product removal.

Recently, the membrane-bound desaturase-like 1-alkene forming enzyme UndB (PFL_0203) with a wider substrate spectrum (C6–C18) was discovered, and it was demonstrated that the UndB had distinguished *in vivo* activity towards 1-alkene synthesis in *E. coli* (Rui et al., 2015). Expression of the membrane-bound UndB in yeast might be toxic to cells, whereas expressing the cytosolic UndA did not show a visible growth arrest (data not shown). UndA, with narrower substrate preference, would not compete for long chain fatty acids that are essential for cell growth. Furthermore, converting toxic

MCFAs to hydrophobic and volatile 1-alkenes which are less toxic or could be readily removed by gas stripping is also a good feature for 1-alkene production.

4. Conclusion

In this study, we engineered yeast to enable the biosynthesis of gasoline or jet fuels range hydrocarbons by introducing the modified FASs from *S. cerevisiae* to supply medium chain fatty acid precursors, and expression of downstream alkane or 1-alkene forming pathways to produce medium chain hydrocarbons. For the two-step synthesis of alkanes, the poor catalytic activities of ADOs and the drain of aldehyde intermediates into alcohols posed a serious obstacle to further improvement of alkane production. We therefore evaluated the direct synthesis of 1-alkenes by decarboxylation of fatty acids, as this avoided the formation of aldehyde intermediates. We showed that the UndA dependent 1-alkene production was much more efficient than the alkane biosynthesis in yeast.

References

Aarts, M. G., Keijzer, C. J., Stiekema, W. J., Pereira, A., 1995. Molecular characterization of the CER1 gene of arabidopsis involved in epicuticular wax biosynthesis and pollen fertility. Plant Cell. 7**,** 2115-2127.

Akhtar, M. K., Turner, N. J., Jones, P. R., 2013. Carboxylic acid reductase is a versatile enzyme for the conversion of fatty acids into fuels and chemical commodities. Proc Natl Acad Sci USA. 110**,** 87-92.

Amaya, J. A., Rutland, C. D., Makris, T. M., 2016. Mixed regiospecificity compromises alkene synthesis by a cytochrome P450 peroxygenase from Methylobacterium populi. J Inorg Biochem. 158**,** 11-16.

Andre, C., Kim, S. W., Yu, X.-H., Shanklin, J., 2013. Fusing catalase to an alkane-producing enzyme maintains enzymatic activity by converting the inhibitory byproduct H2O2 to the cosubstrate O2. Proc Natl Acad Sci USA. 110**,** 3191-3196.

Becker, J., Wittmann, C., 2015. Advanced Biotechnology: Metabolically Engineered Cells for the Bio-Based Production of Chemicals and Fuels, Materials, and Health-Care Products. Angew Chem Int Ed. 54**,** 3328-3350.

Bernard, A., Domergue, F., Pascal, S., Jetter, R., Renne, C., Faure, J.-D., Haslam, R. P., Napier, J. A., Lessire, R., Joubès, J., 2012. Reconstitution of Plant Alkane Biosynthesis in Yeast Demonstrates That Arabidopsis ECERIFERUM1 and ECERIFERUM3 Are Core Components of a Very-Long-Chain Alkane Synthesis Complex. Plant Cell. 24**,** 3106-3118.

Blazeck, J., Garg, R., Reed, B., Alper, H. S., 2012. Controlling promoter strength and regulation in Saccharomyces cerevisiae using synthetic hybrid promoters. Biotechnol Bioeng. 109**,** 2884-2895.

Buijs, N. A., Zhou, Y. J., Siewers, V., Nielsen, J., 2015. Long-chain alkane production by the yeast Saccharomyces cerevisiae. Biotechnol Bioeng. 112**,** 1275-1279.

Cao, Y.-X., Xiao, W.-H., Zhang, J.-L., Xie, Z.-X., Ding, M.-Z., Yuan, Y.-J., 2016. Heterologous biosynthesis and manipulation of alkanes in Escherichia coli. Metab Eng. 38**,** 19-28.

Chen, B., Lee, D.-Y., Chang, M. W., 2015. Combinatorial metabolic engineering of Saccharomyces cerevisiae for terminal alkene production. Metab Eng. 31**,** 53-61.

Choi, Y. J., Lee, S. Y., 2013. Microbial production of short-chain alkanes. Nature. 502**,** 571-574.

Coursolle, D., Lian, J., Shanklin, J., Zhao, H., 2015. Production of long chain alcohols and alkanes upon coexpression of an acyl-ACP reductase and aldehyde-deformylating oxygenase with a bacterial type-I fatty acid synthase in E. coli. Mol Biosyst. 11**,** 2464-2472.

Das, D., Eser, B. E., Han, J., Sciore, A., Marsh, E. N. G., 2011. Oxygen-Independent Decarbonylation of Aldehydes by Cyanobacterial Aldehyde Decarbonylase: A New Reaction of Diiron Enzymes. Angew Chem Int Ed. 50**,** 7148-7152.

Dennig, A., Kuhn, M., Tassoti, S., Thiessenhusen, A., Gilch, S., Bülter, T., Haas, T., Hall, M., Faber, K., 2015. Oxidative Decarboxylation of Short-Chain Fatty Acids to 1-Alkenes. Angew Chem Int Ed. 54**,** 8819-8822.

DiCarlo, J. E., Norville, J. E., Mali, P., Rios, X., Aach, J., Church, G. M., 2013. Genome engineering in Saccharomyces cerevisiae using CRISPR-Cas systems. Nucleic Acids Res. 41**,** 4336-4343.

Edwards, T., 2003. Liquid Fuels and Propellants for Aerospace Propulsion: 1903-2003. J Propul Power. 19**,** 1089-1107.

Eser, B. E., Das, D., Han, J., Jones, P. R., Marsh, E. N. G., 2011. Oxygen-Independent Alkane Formation by Non-Heme Iron-Dependent Cyanobacterial Aldehyde Decarbonylase: Investigation of Kinetics and Requirement for an External Electron Donor. Biochemistry. 50**,** 10743-10750.

Finnigan, W., Thomas, A., Cromar, H., Gough, B., Snajdrova, R., Adams, J. P., Littlechild, J. A., Harmer, N., 2016. Characterization of carboxylic acid reductases as enzymes in the toolbox for synthetic chemistry. ChemCatChem. DOI: 10.1002/cctc.201601249.

Foo, J. L., Susanto, A. V., Keasling, J. D., Leong, S. S. J., Chang, M. W., 2017. Whole-cell biocatalytic and de novo production of alkanes from free fatty acids in Saccharomyces cerevisiae. Biotechnol Bioeng. 114**,** 232-237.

Gajewski, J., Buelens, F., Serdjukow, S., Janszen, M., Cortina, N., Grubmuller, H., Grininger, M., 2017a. Engineering fatty acid synthases for directed polyketide production. Nat Chem Biol. 13**,** 363-365.

Gajewski, J., Pavlovic, R., Fischer, M., Boles, E., Grininger, M., 2017b. Engineering fungal de novo fatty acid synthesis for short chain fatty acid production. Nat Commun. 8**,** 14650.

Gietz, R. D., Schiestl, R. H., 2007. High-efficiency yeast transformation using the LiAc/SS carrier DNA/PEG method. Nat Protoc. 2**,** 31-34.

Gueldener, U., Heinisch, J., Koehler, G. J., Voss, D., Hegemann, J. H., 2002. A second set of loxP marker cassettes for Cre-mediated multiple gene knockouts in budding yeast. Nucleic Acids Res. 30**,** e23.

Hancock, R. D., Galpin, J. R., Viola, R., 2000. Biosynthesis of L-ascorbic acid (vitamin C) by Saccharomyces cerevisiae. FEMS Microbiol Lett. 186**,** 245–250.

Harger, M., Zheng, L., Moon, A., Ager, C., An, J. H., Choe, C., Lai, Y.-L., Mo, B., Zong, D., Smith, M. D., Egbert, R. G., Mills, J. H., Baker, D., Pultz, I. S., Siegel, J. B., 2013. Expanding the Product Profile of a Microbial Alkane Biosynthetic Pathway. ACS Synth Biol. 2**,** 59-62.

Hong, K.-K., Nielsen, J., 2012. Metabolic engineering of Saccharomyces cerevisiae: a key cell factory platform for future biorefineries. Cell Mol Life Sci. 69**,** 2671-2690.

Howard, T. P., Middelhaufe, S., Moore, K., Edner, C., Kolak, D. M., Taylor, G. N., Parker, D. A., Lee, R., Smirnoff, N., Aves, S. J., Love, J., 2013. Synthesis of customized petroleum-replica fuel molecules by targeted modification of free fatty acid pools in Escherichia coli. Proc Natl Acad Sci USA. 110**,** 7636-7641.

Inoue, H., Nojima, H., Okayama, H., 1990. High efficiency transformation of Escherichia coli with plasmids. Gene. 96**,** 23-28.

Jensen, N. B., Strucko, T., Kildegaard, K. R., David, F., Maury, J., Mortensen, U. H., Forster, J., Nielsen, J., Borodina, I., 2014. EasyClone: method for iterative chromosomal integration of multiple genes *Saccharomyces cerevisiae*. FEMS Yeast Res. 14**,** 238–248.

Jia, C., Li, M., Li, J., Zhang, J., Zhang, H., Cao, P., Pan, X., Lu, X., Chang, W., 2015. Structural insights into the catalytic mechanism of aldehyde-deformylating oxygenases. Protein Cell. 6**,** 55-67.

Kallio, P., Pásztor, A., Thiel, K., Akhtar, M. K., Jones, P. R., 2014. An engineered pathway for the biosynthesis of renewable propane. Nat Commun. 5**,** 4731.

Khara, B., Menon, N., Levy, C., Mansell, D., Das, D., Marsh, E. N. G., Leys, D., Scrutton, N. S., 2013. Production of Propane and Other Short-Chain Alkanes by Structure-Based Engineering of Ligand Specificity in Aldehyde-Deformylating Oxygenase. ChemBioChem. 14**,** 1204-1208.

Kourist, R., 2015. A New Class of Enzymes Discovered: A Non-Heme Oxidase Produces Medium-Chain 1-Alkenes. Angew Chem Int Ed. 54**,** 4156-4158.

Kushnirov, V. V., 2000. Rapid and reliable protein extraction from yeast. Yeast. 16**,** 857-860.

Liu, P., Chernyshov, A., Najdi, T., Fu, Y., Dickerson, J., Sandmeyer, S., Jarboe, L., 2013. Membrane stress caused by octanoic acid in Saccharomyces cerevisiae. Appl Microbiol Biotechnol. 97**,** 3239-3251.

Liu, Y., Wang, C., Yan, J., Zhang, W., Guan, W., Lu, X., Li, S., 2014. Hydrogen peroxide-independent production of α-alkenes by OleTJE P450 fatty acid decarboxylase. Biotechnol Biofuels. 7**,** 28.

Looke, M., Kristjuhan, K., Kristjuhan, A., 2011. Extraction of genomic DNA from yeasts for PCR-based applications. BioTechniques. 50**,** 325-328.

Mans, R., van Rossum, H. M., Wijsman, M., Backx, A., Kuijpers, N. G. A., van den Broek, M., Daran-Lapujade, P., Pronk, J. T., van Maris, A. J. A., Daran, J.-M. G., 2015. CRISPR/Cas9: a molecular Swiss army knife for simultaneous introduction of multiple genetic modifications in Saccharomyces cerevisiae. FEMS Yeast Res. 15**,** fov004.

Marsh, E. N. G., Waugh, M. W., 2013. Aldehyde Decarbonylases: Enigmatic Enzymes of Hydrocarbon Biosynthesis. ACS Catal. 3**,** 2515-2521.

Nakahara, K., Ohkuni, A., Kitamura, T., Abe, K., Naganuma, T., Ohno, Y., Zoeller, R. A., Kihara, A., 2012. The Sjögren-Larsson Syndrome Gene Encodes a Hexadecenal Dehydrogenase of the Sphingosine 1-Phosphate Degradation Pathway. Mol Cell. 46**,** 461-471.

Nehlin, J. O., Carlberg, M., Ronne, H., 1991. Control of yeast GAL genes by MIG1 repressor: a transcriptional cascade in the glucose response. EMBO J. 10**,** 3373-3377.

Nielsen, J., 2015. Yeast cell factories on the horizon. Science. 349**,** 1050-1051.

Pannala, V. R., Bhat, P. J., Bhartiya, S., Venkatesh, K. V., 2010. Systems biology of GAL regulon in Saccharomyces cerevisiae. WIRES Syst Biol Med. 2**,** 98-106.

Payet, L.-A., Leroux, M., Willison, J. C., Kihara, A., Pelosi, L., Pierrel, F., 2016. Mechanistic Details of Early Steps in Coenzyme Q Biosynthesis Pathway in Yeast. Cell Chem Biol. 23**,** 1241-1250.

Qiu, Y., Tittiger, C., Wicker-Thomas, C., Le Goff, G., Young, S., Wajnberg, E., Fricaux, T., Taquet, N., Blomquist, G. J., Feyereisen, R., 2012. An insect-specific P450 oxidative decarbonylase for cuticular hydrocarbon biosynthesis. Proc Natl Acad Sci USA. 109**,** 14858-14863.

Reid, R. J. D., Sunjevaric, I., Kedacche, M., Rothstein, R., 2002. Efficient PCR-based gene disruption in *Saccharomyces* strains using intergenic primers. Yeast. 19**,** 319–328.

Rude, M. A., Baron, T. S., Brubaker, S., Alibhai, M., Del Cardayre, S. B., Schirmer, A., 2011. Terminal Olefin (1-Alkene) Biosynthesis by a Novel P450 Fatty Acid Decarboxylase from Jeotgalicoccus Species. Appl Environ Microbiol. 77**,** 1718-1727.

Rui, Z., Harris, N. C., Zhu, X., Huang, W., Zhang, W., 2015. Discovery of a Family of Desaturase-Like Enzymes for 1-Alkene Biosynthesis. ACS Catal. 5**,** 7091-7094.

Rui, Z., Li, X., Zhu, X., Liu, J., Domigan, B., Barr, I., Cate, J. H. D., Zhang, W., 2014. Microbial biosynthesis of medium-chain 1-alkenes by a nonheme iron oxidase. Proc Natl Acad Sci USA. 111**,** 18237-18242.

Schirmer, A., Rude, M. A., Li, X., Popova, E., del Cardayre, S. B., 2010. Microbial biosynthesis of alkanes. Science. 329**,** 559-562.

Shao, Y. Y., Seib, P. A., Kramer, K. J., Van Galen, D. A., 1993. Synthesis and properties of D-erythroascorbic acid and its vitamin C activity in the tobacco hornworm (Manduca sexta). J Agric Food Chem. 41**,** 1391-1396.

Shao, Z., Zhao, H., Zhao, H., 2009. DNA assembler, an in vivo genetic method for rapid construction of biochemical pathways. Nucleic Acids Res. 37**,** e16.

Sheppard, M. J., Kunjapur, A. M., Prather, K. L. J., 2016. Modular and selective biosynthesis of gasoline-range alkanes. Metab Eng. 33**,** 28-40.

Slaymaker, I. M., Gao, L., Zetsche, B., Scott, D. A., Yan, W. X., Zhang, F., 2016. Rationally engineered Cas9 nucleases with improved specificity. Science. 351**,** 84-88.

Song, X., Yu, H., Zhu, K., 2016. Improving alkane synthesis in Escherichia coli via metabolic engineering. Appl Microbiol Biotechnol. 100**,** 757-767.

Stefely, J. A., Kwiecien, N. W., Freiberger, E. C., Richards, A. L., Jochem, A., Rush, M. J. P., Ulbrich, A., Robinson, K. P., Hutchins, P. D., Veling, M. T., Guo, X., Kemmerer, Z. A., Connors, K. J., Trujillo, E. A., Sokol, J., Marx, H., Westphall, M. S., Hebert, A. S., Pagliarini, D. J., Coon, J. J., 2016. Mitochondrial protein functions elucidated by multi-omic mass spectrometry profiling. Nat Biotechnol. 34**,** 1191-1197.

Warui, D. M., Li, N., Nørgaard, H., Krebs, C., Bollinger, J. M., Booker, S. J., 2011. Detection of Formate, Rather than Carbon Monoxide, As the Stoichiometric Coproduct in Conversion of Fatty Aldehydes to Alkanes by a Cyanobacterial Aldehyde Decarbonylase. J Am Chem Soc. 133**,** 3316-3319.

Xu, P., Qiao, K., Ahn, W. S., Stephanopoulos, G., 2016. Engineering Yarrowia lipolytica as a platform for synthesis of drop-in transportation fuels and oleochemicals. Proc Natl Acad Sci USA. 113**,** 10848-10853.

Yan, H., Wang, Z., Wang, F., Tan, T., Liu, L., 2016. Biosynthesis of chain-specific alkanes by metabolic engineering in Escherichia coli. Eng Life Sci. 16**,** 53-59.

Yan, J., Liu, Y., Wang, C., Han, B., Li, S., 2015. Assembly of lipase and P450 fatty acid decarboxylase to constitute a novel biosynthetic pathway for production of 1-alkenes from renewable triacylglycerols and oils. Biotechnol Biofuels. 8**,** 34.

Zachos, I., Ga, Bauer, D., Sieber, V., Hollmann, F., Kourist, R., 2015. Photobiocatalytic decarboxylation for olefin synthesis. Chem Commun. 51**,** 1918-1921.

Zhang, J., Lu, X., Li, J.-J., 2013. Conversion of fatty aldehydes into alk (a/e)nes by in vitro reconstituted cyanobacterial aldehyde-deformylating oxygenase with the cognate electron transfer system. Biotechnol Biofuels. 6**,** 86.

Zhou, Y. J., Buijs, N. A., Zhu, Z., Gómez, D. O., Boonsombuti, A., Siewers, V., Nielsen, J., 2016a. Harnessing Yeast Peroxisomes for Biosynthesis of Fatty-Acid-Derived Biofuels and Chemicals with Relieved Side-Pathway Competition. J Am Chem Soc. 138**,** 15368-15377.

Zhou, Y. J., Buijs, N. A., Zhu, Z., Qin, J., Siewers, V., Nielsen, J., 2016b. Production of fatty acid-derived oleochemicals and biofuels by synthetic yeast cell factories. Nat Commun. 7**,** 11709.

Zhou, Y. J., Gao, W., Rong, Q., Jin, G., Chu, H., Liu, W., Yang, W., Zhu, Z., Li, G., Zhu, G., Huang, L., Zhao, Z. K., 2012. Modular pathway engineering of diterpenoid synthases and the mevalonic acid pathway for miltiradiene production. J Am Chem Soc. 134**,** 3234–3241.

Zhu, Z., Zhou, Y. J., Krivoruchko, A., Grininger, M., Zhao, Z. K., Nielsen, J., 2017. Expanding the product portfolio of fungal type I fatty acid synthases. Nat Chem Biol. 13**,** 360-362.

Acknowledgment

This work was financially supported by the Novo Nordisk Foundation, the Knut and Alice Wallenberg Foundation, Vetenskapsrådet and Total New Energy. We thank the Chalmers Mass Spectrometry Infrastructure for assistance with GC/MS analysis